NACA TN No. 1881

NATIONAL ADVISORY COMMITTEE FOR AERONAUTICS

TECHNICAL NOTE

No. 1881

COMPARISON OF PITCHING MOMENTS OBTAINED DURING SEAPLANE LANDINGS WITH VALUES PREDICTED BY HYDRODYNAMIC IMPACT THEORY

By Gilbert A. Haines

Langley Aeronautical Laboratory
Langley Air Force Base, Va.

Washington
May 1949

NATIONAL ADVISORY COMMITTEE FOR AERONAUTICS

TECHNICAL NOTE NO. 1881

COMPARISON OF PITCHING MOMENTS OBTAINED DURING SEAPLANE LANDINGS WITH VALUES PREDICTED BY HYDRODYNAMIC IMPACT THEORY

By Gilbert A. Haines

SUMMARY

Pitching moments and center-of-pressure locations obtained from a landing investigation in smooth water of a conventional flying boat have been compared with the values predicted by general hydrodynamic impact theory to determine the applicability of the theory to actual seaplane landings. Landings were generally moderate and covered as wide a range of trim and velocities as practical.

The experimental center-of-pressure location was in reasonable agreement with the theoretical value of approximately one-third the wetted keel length forward of the step.

The experimental pitching moments for impacts in which only the V-shaped part of the hull was immersed were in reasonable agreement with theoretical values. For impacts in which the chine flare was immersed the experimental pitching moments were greater than the theoretical values. Diving rotation decreased the experimental pitching moment during the early part of the impact when the center of pressure was aft of the center of gravity and increased the pitching moment when the center of pressure was forward of the center of gravity.

INTRODUCTION

A general hydrodynamic theory (references 1 to 5) for seaplane impacts has been substantiated for a wide range of conditions by model tests in the Langley impact basin. In order to investigate the applicability of theory and model tests to actual seaplane impacts, a full-scale landing investigation was conducted in smooth water with a seaplane having a conventional hull. The actual landings differed from the controlled landings in that the wing lift was not equal to the weight of the airplane and varied throughout the impact, the trim was not constant throughout the impact, and the airplane had an afterbody and a pulled-up bow.

In the course of the investigation, data were obtained for the determination of the over-all load, load distribution, pitching moment, and

center-of-pressure location. The over-all loads have been compared in reference 6 with the loads predicted by general hydrodynamic impact theory. The present paper gives the maximum pitching moments and time histories of pitching moments obtained during forebody impacts and compares them with pitching moments predicted by the theory. Time histories of the experimental ratio of the location of center of pressure to wetted keel length and the experimental ratios at time of maximum moment are compared with the theoretical values.

SYMBOLS

B	pertaining to instant at which water line reached pulled-up-bow region
C	pertaining to instant at which water line reached curved-chine area
g	acceleration due to gravity, 32.2 feet per second per second
I	pitching moment of inertia, slug-feet square
l	wetted keel length, feet
M_s	pitching moment about step, pound-feet
n_{l_k}	impact load factor normal to keel, g units
p	longitudinal distance between step and center of pressure, feet
V_h	horizontal velocity of seaplane relative to water, feet per second
V_v	vertical velocity of step relative to water, feet per second
W	weight of seaplane, pounds
α	angular acceleration, radians per second per second
β	angle of dead rise, degrees
γ	flight-path angle, degrees $\left(\tan^{-1}\frac{V_v}{V_h}\right)$
ρ	mass density of water, 1.972 slugs per cubic foot
τ	trim, degrees
ω	angular pitching velocity, degrees per second

Dimensionless variables:

C_{m_s} pitching-moment coefficient at step $\left(\dfrac{M_s}{V_{v_o}^2 \frac{W}{g} \frac{\phi_1(A)}{\phi(A)} \frac{1}{\sin \tau \cos \tau}}\right)$

κ approach parameter $\left(\dfrac{\sin \tau_o \cos(\tau_o + \gamma_o)}{\sin \gamma_o}\right)$

$f(\beta)$ dead-rise correction to water mass $\left(\frac{\pi}{2\beta} - 1;\ \beta \text{ expressed in radians}\right)$

$\phi(A)$ end-loss correction to water mass and total load $\left(1 - \dfrac{\tan \tau}{2 \tan \beta}\right)$

$\phi_1(A)$ end-loss correction to pitching moment; assumed equal to $\phi(A)$

Subscripts:

e experimental

c computed

t theoretical

o at time of water contact

max maximum

APPARATUS AND EQUIPMENT

The airplane used in the flight tests was a conventional flying boat with a gross weight of about 20,000 pounds and is shown in figure 1. Pertinent information about the airplane is given in table I. The hull has a V-bottom that has an angle of dead rise of 20° and terminates in transverse curvature in the region of the chine (chine flare). The drawing of the hull lines is shown in figure 2.

Measurements were made to obtain such basic quantities as trim, vertical and horizontal velocities, normal and angular accelerations, and wetted keel lengths for principal impacts during each landing.

The instrumentation used to obtain these measurements included a gyroscopic trim recorder, a standard NACA optical-recording three-component accelerometer having a natural frequency of about 19 cycles per second that was also used to obtain wing lift at time of contact, and an electrical angular accelerometer of the inductive-bridge type having a natural frequency of approximately 22 cycles per second. The vertical velocity of the step was determined from records obtained from a motion-picture camera mounted near the wing tip, which photographed a rod that contacted the water below the forebody step. This method is explained in detail in appendix A of reference 6. The horizontal velocity relative to the water was obtained from an inductive-type pressure gage mounted in a tube in such a manner as to measure the dynamic pressure of the water at the same level as the keel near the forebody step. The wetted keel lengths were obtained from the time of immersion of electrical pressure gages and water contacts mounted flush in the hull bottom. The water contacts consisted of small spark plugs, each of which closed an electrical circuit when wet. The locations of the instruments in the flying boat are shown in table II and in figures 3 and 4.

TEST PROCEDURE

Landings were generally moderate and were made in smooth water. The initial values of vertical velocities ranged from 1.1 to 9.1 feet per second, horizontal velocities from 82 to 126 feet per second, flight-path angles from 0.5° to 4.82°, trim from 3.0° to 8.1°, angular velocities from −6.5° per second to 1.0° per second, and wing lift from 0.7g to 1g.

The impacts presented in this paper were frequently the second or third impact in the landing, as noted in table III.

PRECISION OF MEASUREMENTS

The estimated accuracies of reported experimental data based on both instrument and reading error are as follows:

V_h, feet per second	±4
V_v, feet per second	±1
τ, degrees	±1/4
n_{i_k}, g units	±0.3
α, radians per second per second	±1/4
l, feet	±0.5

ANALYSIS AND REDUCTION OF DATA

Theoretical Background

The theoretical investigation presented in references 3 and 4 showed that the motion, hydrodynamic loads, and pitching moments experienced by V-bottom seaplanes during a step-landing impact could be represented by dimensionless generalized variables that take into account such factors as angle of dead rise, weight, trim angle, and initial velocity. The variation of these variables during an impact is determined by the magnitude of another generalized variable called the approach parameter κ, which is dependent only on the trim angle and flight-path angle at time of contact.

The theoretical pitching-moment investigation involves the following assumptions: (1) The hull consists of only a forebody with a V-bottom of indefinite beam (such that the chines do not become immersed) and straight keel and with a constant cross section, (2) the trim remains constant throughout the impact, and (3) the wing lift is equal to the weight of the airplane and is constant throughout the impact. Among the theoretical results presented in reference 4 is the conclusion that for the normal range of impact conditions the center of pressure is located at a distance only slightly more than one-third the wetted keel length forward of the step.

The conditions in the full-scale landings differed from the assumptions made in the theoretical investigation by the presence of an afterbody and a pulled-up bow and by the fact that the amount of trim and wing lift varied throughout the impact. The presence of chine flare on the forebody hull of the seaplane could have been included in the theoretical assumptions by use of reference 2, but the additional complexity was not believed to be warranted.

Determination of the Center of Pressure

The experimental center-of-pressure location from the step was obtained by dividing the experimental pitching moment about the step by the corresponding normal load.

The experimental ratio of center of pressure to wetted keel length was obtained by dividing the location of the center of pressure from the step by the corresponding wetted keel length.

In the calculations of the computed pitching moment, the center-of-pressure location is assumed to be one-third the experimental wetted keel length.

Determination of Pitching Moments

Experimental values of the full-scale pitching moment were obtained from the product of the measured angular acceleration and the pitching moment of inertia of the airplane about the center of gravity. Since the center of gravity is not located at the step (2.60 ft forward), the experimental pitching moment was transferred to the step by means of the equation

$$M_{s_e} = I\alpha + n_{i_k} \times W \times 2.60$$

This equation neglects changes in pitching moment due to changes in aerodynamic lift.

In order to evaluate the theoretical center-of-pressure locations, computed values of the full-scale pitching moment were obtained by multiplying the normal load by a moment arm of one-third the wetted keel length.

RESULTS AND DISCUSSION

The basic data obtained in the present investigation are presented in table III. Included in this table are vertical velocity, horizontal velocity, flight-path angle, trim, angular velocity, and wing lift. All these data were taken at time of water contact.

Two typical acceleration records are presented in figure 5 for runs 5 and 7.

A comparison of the ratio of experimental center of pressure to wetted keel length at maximum pitching moment with the theoretical ratio is presented in figure 6. These values are plotted against the approach parameter κ and are classified as to the type of impact. These experimental ratios are presented in table III.

A comparison of the maximum experimental and theoretical pitching-moment coefficients about the step is presented in figure 7. The coefficients are plotted against κ and are classified as to the type of impact. The maximum experimental pitching moments for these runs are presented in table III. In figures 8 and 9 time histories of the ratio of center of pressure to wetted keel length and experimental and computed pitching moments about the step are compared with those predicted by the theory. Also in figure 8 the normal load is compared with values predicted by the theory and the effect of initial rotation and chine immersion on loads and pitching moments is shown.

Center of Pressure

In figures 6, 8, and 9 the experimental ratios of center of pressure to wetted keel length appear to be in reasonable agreement with the

theoretical ratio. The importance of this agreement is that if the correct load and draft are known, a reasonably accurate moment can be obtained by using a moment arm equal to one-third the wetted keel length.

For the runs in which the chines were immersed, the experimental values showed the least agreement with the theoretical values, as might reasonably be expected. This result is due to the fact that, because the airplane had a definite beam and the chine became immersed, the wetted area was made up of a triangle and a rectangle instead of only a triangle and therefore the center of pressure was somewhat greater than one-third the wetted keel length from the step. Immersion of the chine flare would tend to move the center of pressure rearward; whereas chine immersion would tend to move the center of pressure forward.

For the runs in which the pulled-up bow was immersed the chines were also immersed. However, for run 12, which was at a low trim, the triangular wetted area was so much larger than the rectangular area that the center of pressure was not moved appreciably from the one-third value. In run 13 the chine flare was involved appreciably but the chines were not; therefore the effect was to move the center of pressure rearward toward the position of one-third the wetted keel length.

The effect of initial rotation on the center-of-pressure location of one-third the wetted keel length does not appear to be appreciable.

Pitching Moments

No chine immersion.- In most moderate landings the measurements of angular accelerations and wetted keel lengths were too small to be obtained or determined accurately. Therefore, only runs 1, 2, and 3 are considered for the case where the chine curvature was not immersed at time of maximum load. In run 1 the angular acceleration was too small to be read accurately; therefore only the computed moment is considered for this particular impact.

In figure 7, these three runs, which are represented by the circles, are seen to lie reasonably close to the theoretical line. The time histories of the experimental and computed pitching moments for runs 2 and 3 are shown in figures 9 and 8, respectively. The experimental values are observed to be in good agreement with the theoretical curve, the maximum experimental and maximum computed values being slightly higher. The other runs shown in figures 8 and 9 indicate that, prior to the time that the chine flare is immersed, the pitching moments are in reasonable agreement with those predicted by theory.

Chine immersion.- The impacts that are considered as having chine immersion are impacts in which the chine flare becomes immersed prior to the time of maximum load.

In figure 7 the values of maximum pitching-moment coefficient for the case of chine immersion represented by squares are seen to be considerably greater than the theoretical values. Of these impacts the one with no initial rotation lies closest to the theoretical curve. Runs 3 and 5 in figure 8 show the effect of chine immersion on the agreement of the loads and pitching moments with the theoretical values.

The effect of chine flare was an increase in the local pressure in the area adjacent to the chines and thus an increase in the total load. Chine immersion tended to relieve the pressure adjacent to the chine and therefore tended to decrease the total load. The net effect, however, appears to be an increase in the load, which caused an increase in the pitching moment.

Bow and chine immersion.- In the extreme case in which the bow region becomes immersed, as represented by the triangles in figure 7, the points lie closer to the theoretical curve than the ones in which only the chines are involved. In run 12 (see fig. 9), the maximum moment was actually less than the theoretical value because the arm based on the wetted length was less than it would have been had the straight part of the keel extended forward to a greater length. Furthermore, the normal load in this impact was less than for the ideal float with straight keel.

In run 13 the pulled-up bow is not involved appreciably and the normal load is slightly less than the theoretical load. However, because the draft is greater than the theoretical value, the moment arm is larger and therefore the pitching moment is larger.

Rotation.- The effect of diving rotation is a decrease in the load when the center of pressure is aft of the center of gravity. This decrease in load is due to the fact that the after portion of the float is at a lower effective vertical velocity because of the rotation about the center of gravity. The wetted keel lengths are increased since the float is pitching down. During the early part of the impact, as shown for runs 5 and 7 in figure 8, the decrease in load is greater than the increase in wetted keel length and the resulting pitching moment is less than the theoretical fixed-trim values. When the center of pressure is forward of the center of gravity, the load and the wetted keel lengths are increased, and the forward portion of the float has a higher effective vertical velocity because of the pitching-down rotation.

The effects of pitching-up rotation are the reverse of the effects of diving rotation.

SUMMARY OF RESULTS

A landing investigation was conducted on a full-scale conventional flying boat and the analysis of the data leads to the following results:

1. The center-of-pressure location was in reasonable agreement with the theoretical value of approximately one-third the wetted keel length. As might be expected, for the impacts in which the chines were immersed, the experimental values showed the least agreement with the theoretical values.

2. The pitching moments for impacts in which only the V-shaped part of the forebody was immersed were in reasonable agreement with the values predicted by the hydrodynamic impact theory.

3. The effect of the immersion of the chine flare was an increase in the experimental pitching moments over the theoretical values that were based on the assumption of straight V-bottom. This increase was due to the increased local pressure in the region adjacent to the chines, which resulted in an increase in the over-all load.

4. The effects of diving rotation were as follows:

(a) During the early part of the impact when the center of pressure was aft of the center of gravity the pitching moment was decreased. The decrease in normal load was greater than the increase in wetted length.

(b) When the center of pressure was forward of the center of gravity the pitching moment was increased. The normal load and the wetted length were also increased.

Langley Aeronautical Laboratory
National Advisory Committee for Aeronautics
Langley Air Force Base, Va., March 23, 1949

REFERENCES

1. Mayo, Wilbur L.: Analysis and Modification of Theory for Impact of Seaplanes on Water. NACA Rep. No. 810, 1945.

2. Milwitzky, Benjamin: A Theoretical Investigation of Hydrodynamic Impact Loads on Scalloped-Bottom Seaplanes and Comparisons with Experiment. NACA Rep. No. 867, 1947.

3. Milwitzky, Benjamin: A Generalized Theoretical and Experimental Investigation of the Motions and Hydrodynamic Loads Experienced by V-Bottom Seaplanes during Step-Landing Impacts. NACA TN No. 1516, 1948.

4. Milwitzky, Benjamin: A Generalized Theoretical Investigation of the Hydrodynamic Pitching Moments Experienced by V-Bottom Seaplanes during Step-Landing Impact and Comparisons with Experiment. NACA TN No. 1630, 1948.

5. Benscoter, Stanley U.: Impact Theory for Seaplane Landings. NACA TN No. 1437, 1947.

6. Steiner, Margaret F.: Comparison of Over-All Impact Loads Obtained during Seaplane Landing Tests with Loads Predicted by Hydrodynamic Theory. NACA TN No. 1781, 1949.

TABLE I

GENERAL INFORMATION ABOUT FLYING BOAT USED IN FLIGHT TESTS

Normal gross weight, lb	19,000
Approximate flying weight during tests, lb	20,000
Stalling speed (flaps down), knots	56
Wing span, ft	86
Wing chord at root, ft	11.5
Mean aerodynamic chord, ft	9.8
Wing area, sq ft	780.6
Center-of-gravity positions	
Percent mean aerodynamic chord	31.9
Forward of step, ft	2.6
Beam of hull, ft	8.33
Distance from main step to bow, ft	21.25
Moment of inertia, slug-ft^2	48,137

TABLE II

SPECIFIC LOCATION OF INSTRUMENTS

[See fig. 3]

Instrument	Type	Location in airplane (Referred to c.g. or point of step)
1	NACA optical-recording three-component accelerometer	6 in. forward, 3 in. below, 8 in. to starboard of c.g.
2	Electrical angular accelerometer	4 in. forward, 3 in. below, 6 in. to starboard of c.g.
3	Gyroscopic trim recorder	12 in. aft, 60 in. below, 20 in. to port of c.g.
4	Pressure gages and water contacts	(See fig. 4.)
5	Water-speed pressure gage	15 in. forward, axis parallel to keel, 11 in. to starboard of point of step
6	Vertical-displacement indicator	Pivot 13.2 in. aft, 4.4 in. above, 4 in. to port of point of step
7	Wing camera	30 in. forward, 146 in. above, 409 in. to starboard of point of step
8	Water-contact indicator (forebody)	Point of step

TABLE III

FULL-SCALE PITCHING-MOMENT DATA

Run	V_{v_o} (ft/sec)	V_{h_o} (ft/sec)	γ_o (deg)	τ_o (deg)	ω_o (deg/sec)	κ	n_{i_k} (g)	α (radians/sec^2)	$M_{s_{max}}$ (ft)	p/l	Wing lift at contact (g)	Impact
1	1.1	126	0.50	3.6	−0.7	7.18	0.16	-----	6,750	-----	1.0	2
2	7.5	83	4.82	6.2	−6.7	1.18	1.20	0.728	97,000	0.344	.8	3
3	1.3	112	.66	7.6	1.0	11.36	.25	−.166	4,800	.320	1.0	1
4	4.0	99	2.31	5.2	−3.5	2.23	.96	.463	75,500	.364	.7	2
5	4.0	106	2.16	5.4	0	2.48	.80	.312	56,400	.391	1.0	1
6	3.5	90	2.23	5.7	−4.7	2.53	.93	.596	76,000	.329	.8	2
7	4.6	95	2.77	6.0	−4.9	2.14	1.16	.563	87,100	.349	.8	2
8	4.5	83	3.10	6.0	−2.8	1.91	1.14	.532	84,400	.324	.7	3
9	3.25	89	2.09	6.4	−1.1	3.02	1.04	.200	63,300	.368	.8	2
10	3.5	96	2.09	7.5	−4.4	3.53	.98	.133	61,880	.360	.8	2
11	3.25	82	2.27	8.1	−3.0	3.50	.86	.249	56,400	.345	.7	3
12	9.1	98	5.30	3.0	−6.0	.56	1.71	2.450	206,400	.335	.8	2
13	7.5	94	4.56	5.7	−5.0	1.23	1.60	1.260	143,200	.332	.8	2

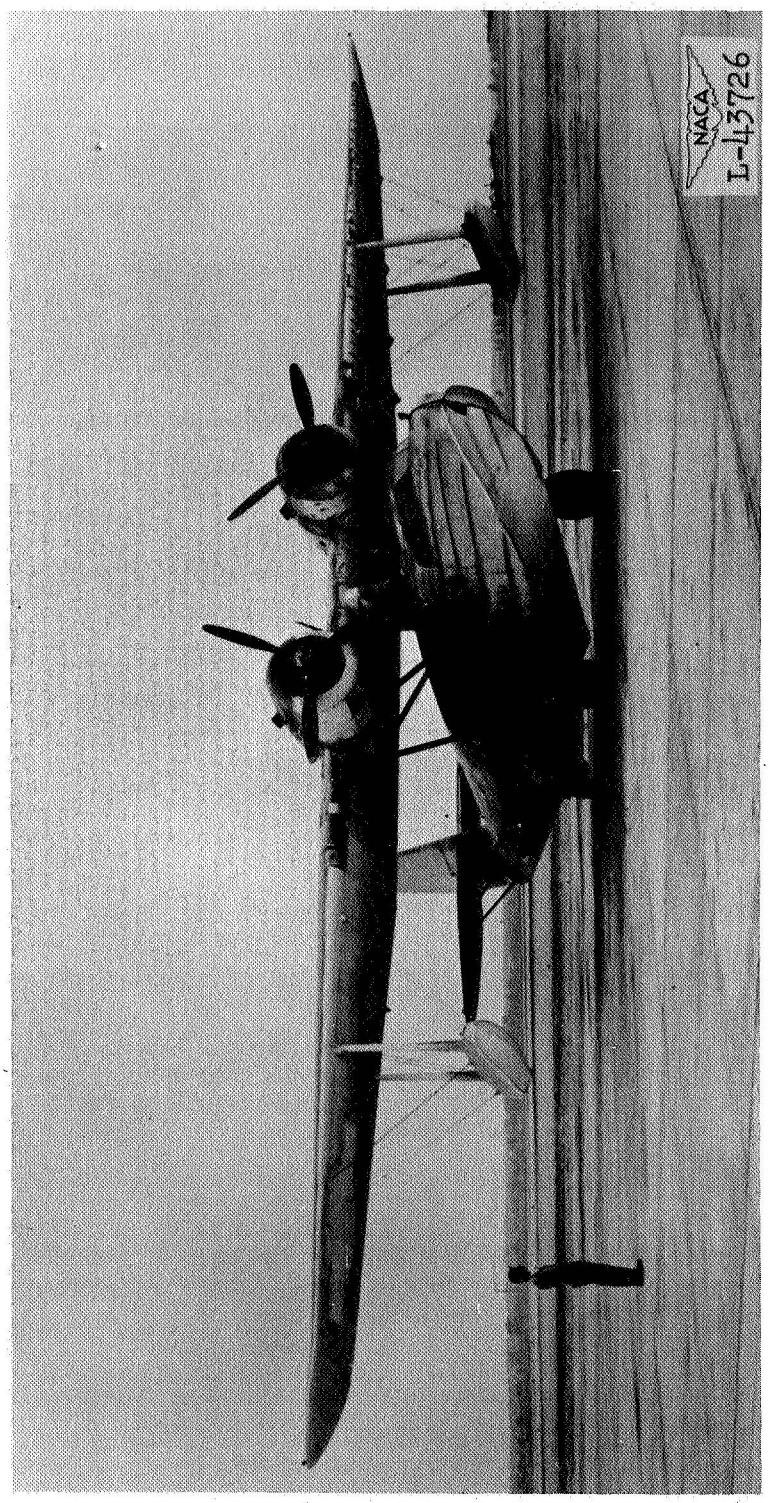

Figure 1.- Flying boat used in landing investigation.

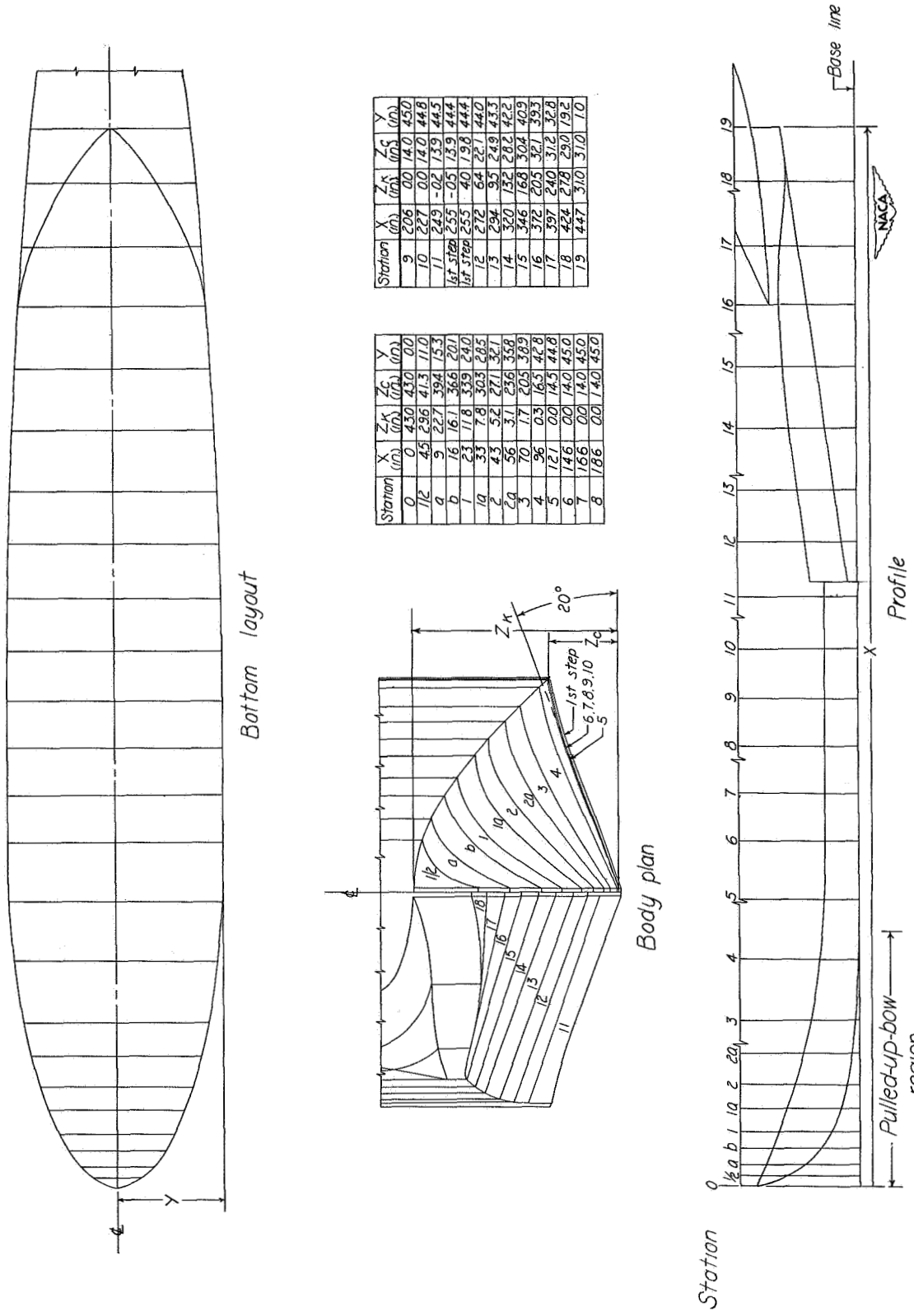

Station	X (in.)	Zk (in.)	Zc (in.)	Y (in.)
0	0	430	430	00
1/2	45	296	41.3	11.0
a	9	22.7	394	153
b	16	16.1	366	201
1	23	11.8	339	240
1a	33	7.8	303	285
2	43	5.2	271	321
2a	56	3.1	236	358
3	70	1.7	205	389
4	96	0.3	165	428
5	121	0.0	145	448
6	146	0.0	140	450
7	166	0.0	140	450
8	186	0.0	140	450

Station	X (in.)	Zk (in.)	Zc (in.)	Y (in.)
9	206	0.0	140	450
10	227	0.0	140	448
11	249	-0.2	139	445
1st step	255	-0.5	139	444
1st step	255	.40	198	444
12	272	6.4	221	440
13	294	9.5	249	433
14	320	13.2	282	422
15	346	16.8	304	409
16	372	20.5	321	393
17	397	24.0	312	328
18	424	27.8	290	192
19	447	31.0	310	10

Figure 2.- Hull lines of flying boat used in landing investigation.

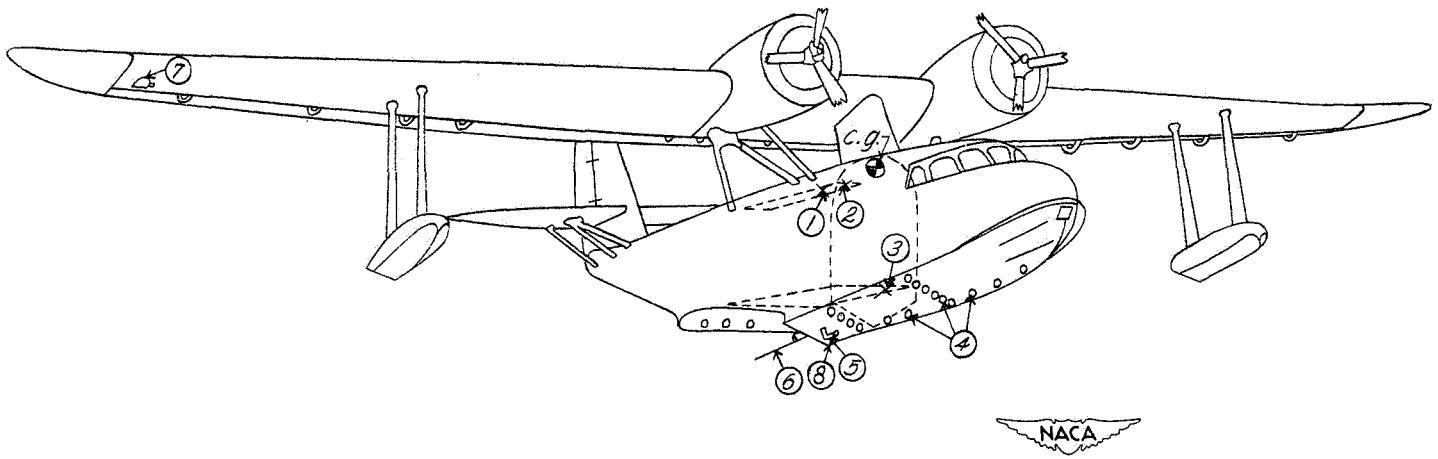

1. NACA optical-recording three-component accelerometer
2. Electrical angular accelerometer
3. Gyroscopic trim recorder
4. Pressure gages and water contacts
5. Water-speed pressure gage
6. Vertical-displacement indicator
7. Wing camera
8. Water-contact indicator (forebody)

Figure 3.- Location of instruments in the flying boat.

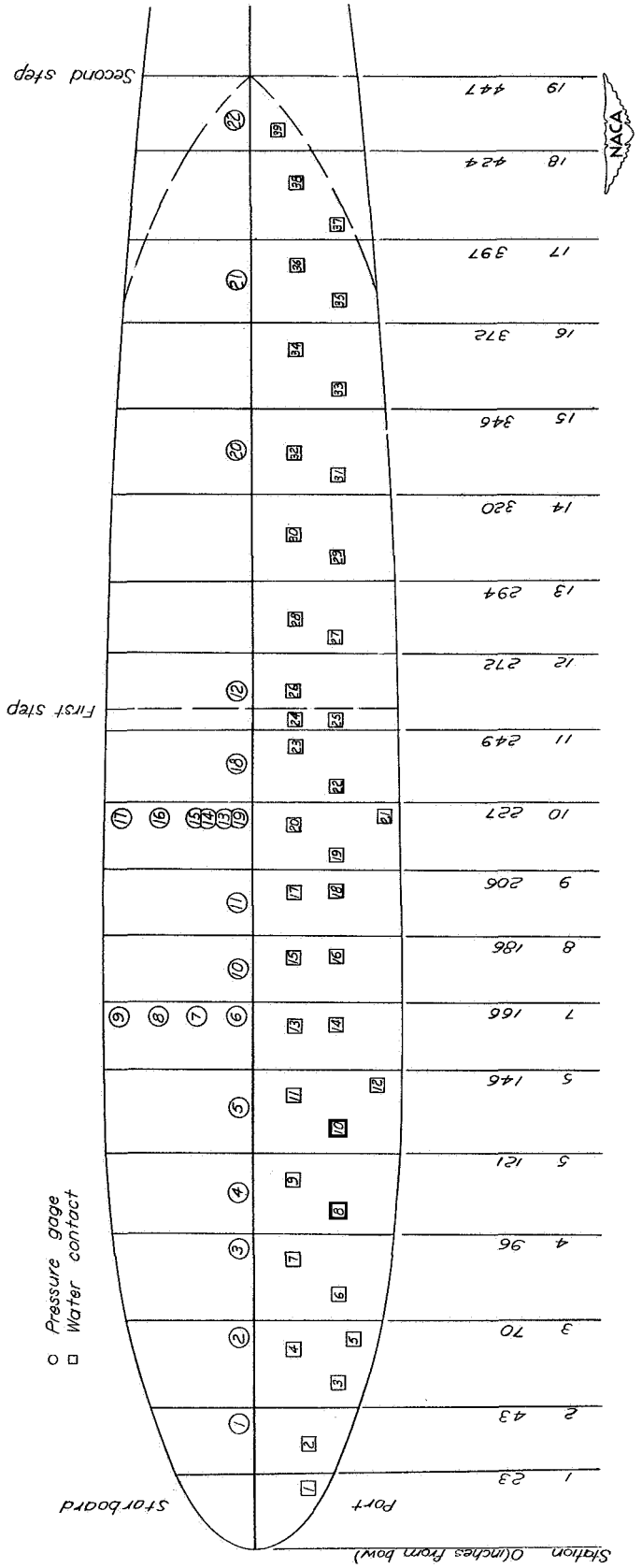

Figure 4.- Location of pressure gages and water contacts in hull bottom.

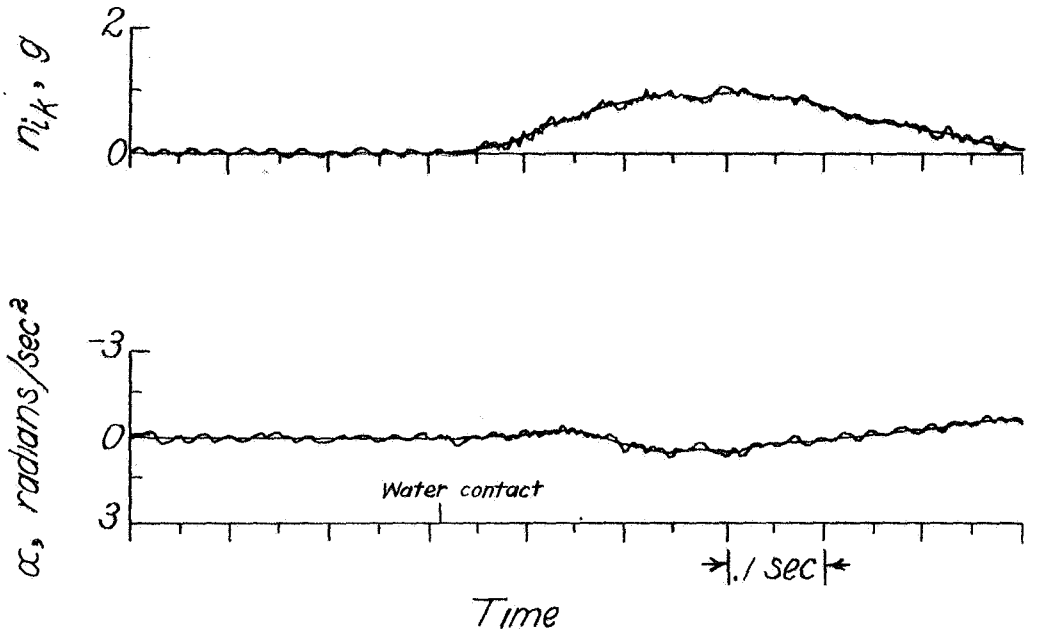

(a) Normal and angular acceleration for run 7.

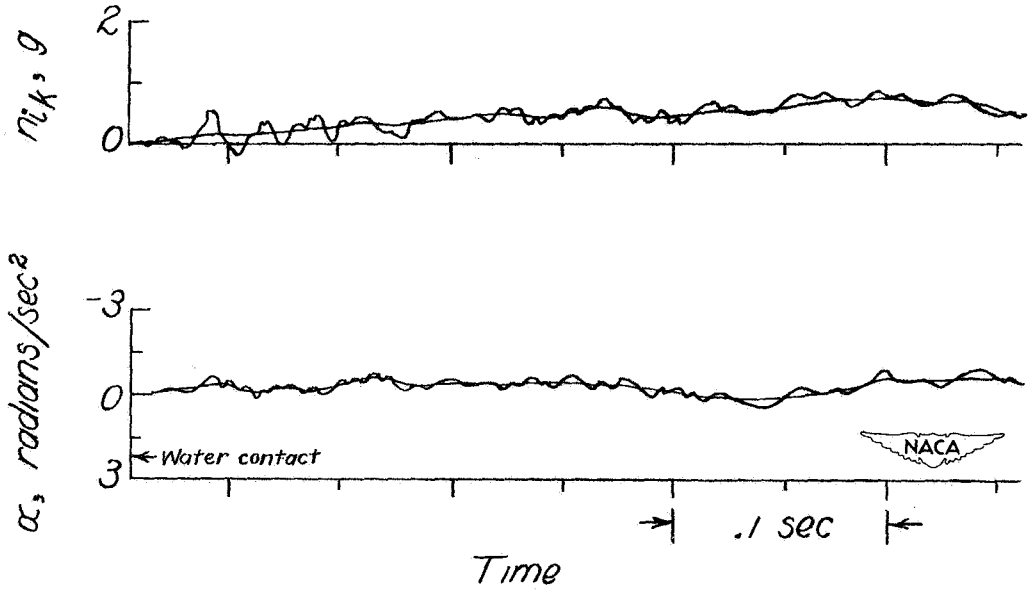

(b) Normal and angular acceleration for run 5.

Figure 5.- Typical acceleration records showing fairing through oscillation.

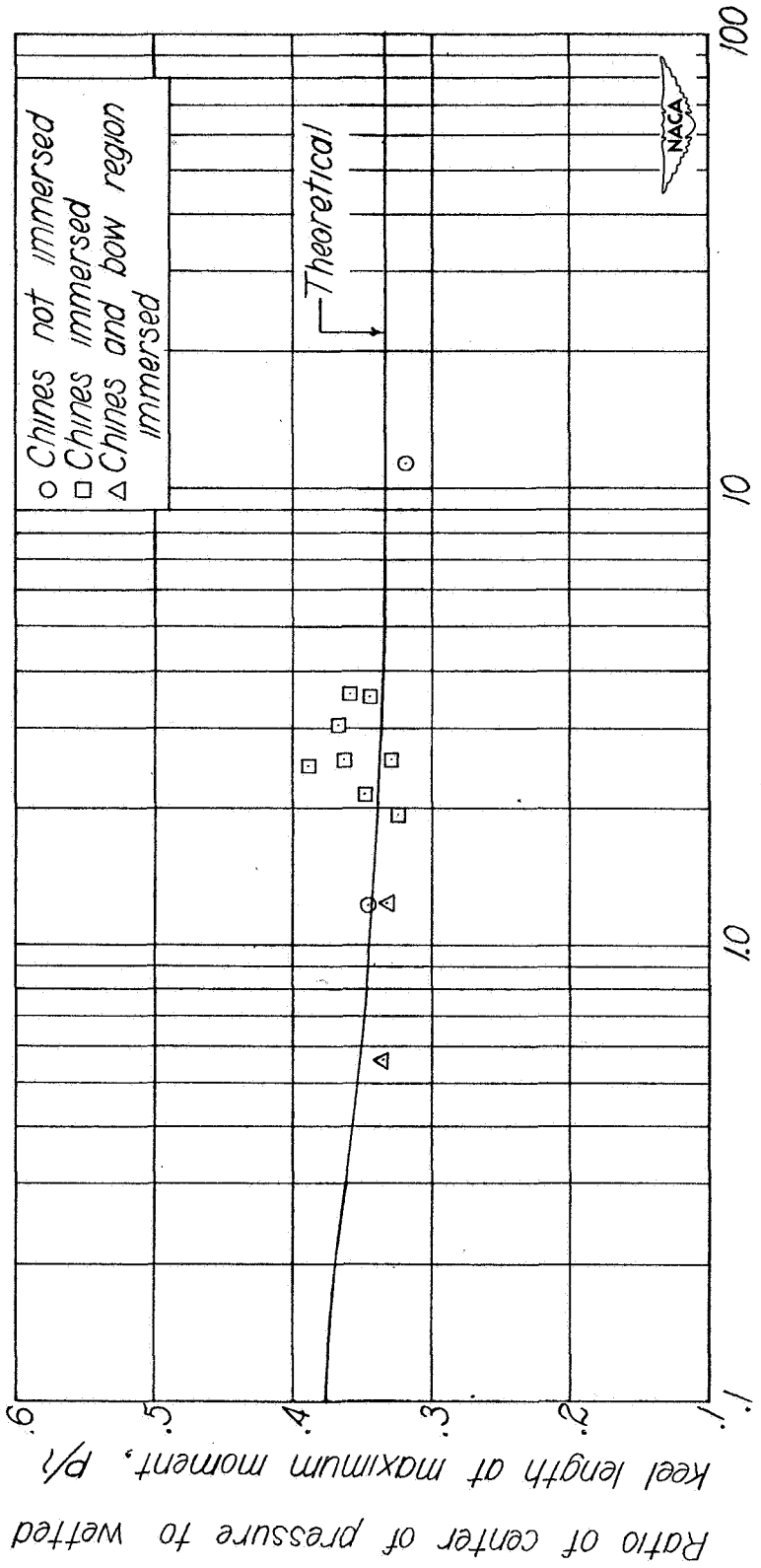

Figure 6.- Comparison of experimental and theoretical ratio of center of pressure to wetted keel length at maximum moment.

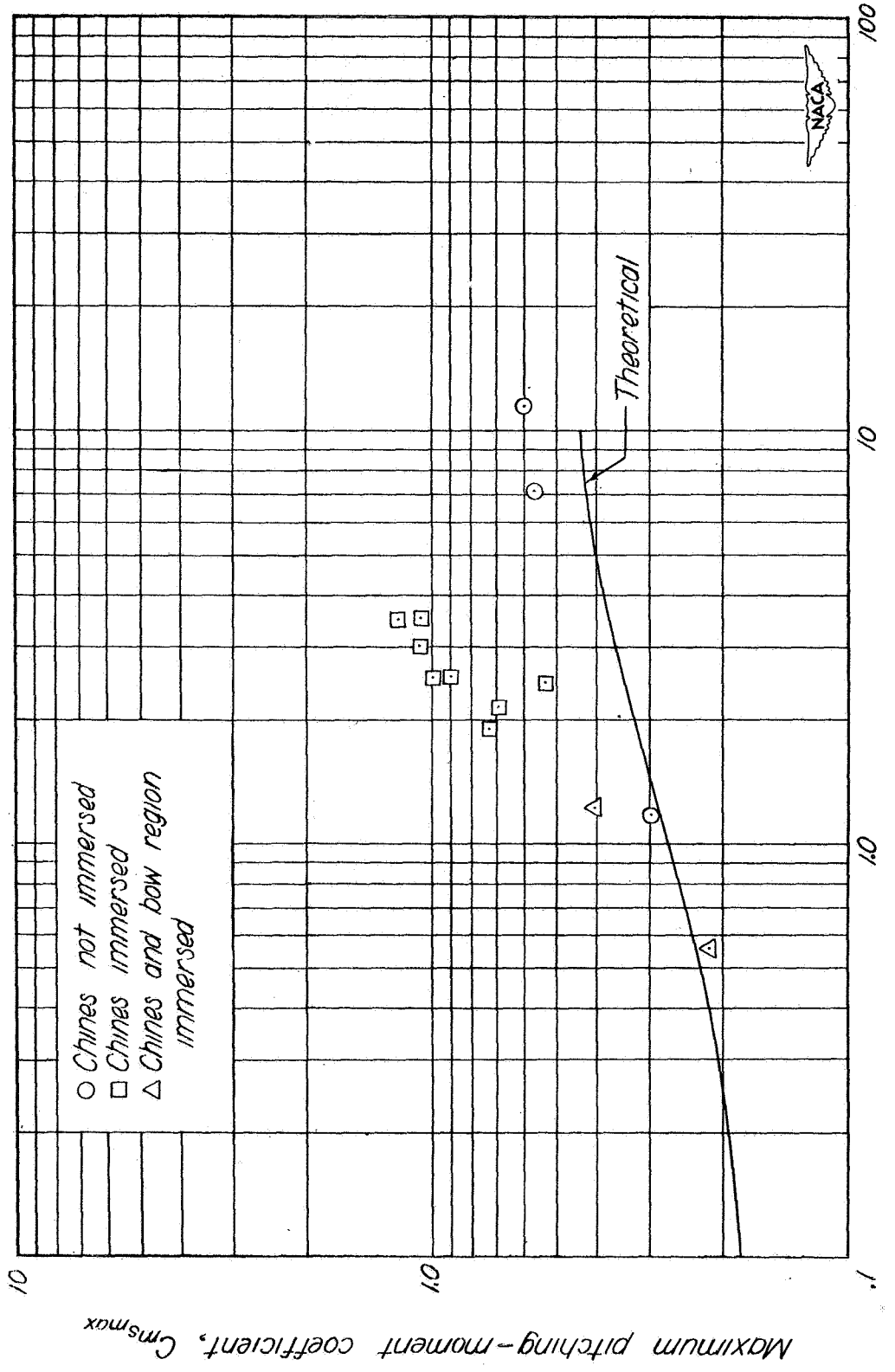

Figure 7.- Comparison of maximum experimental and theoretical pitching-moment coefficients about the step.

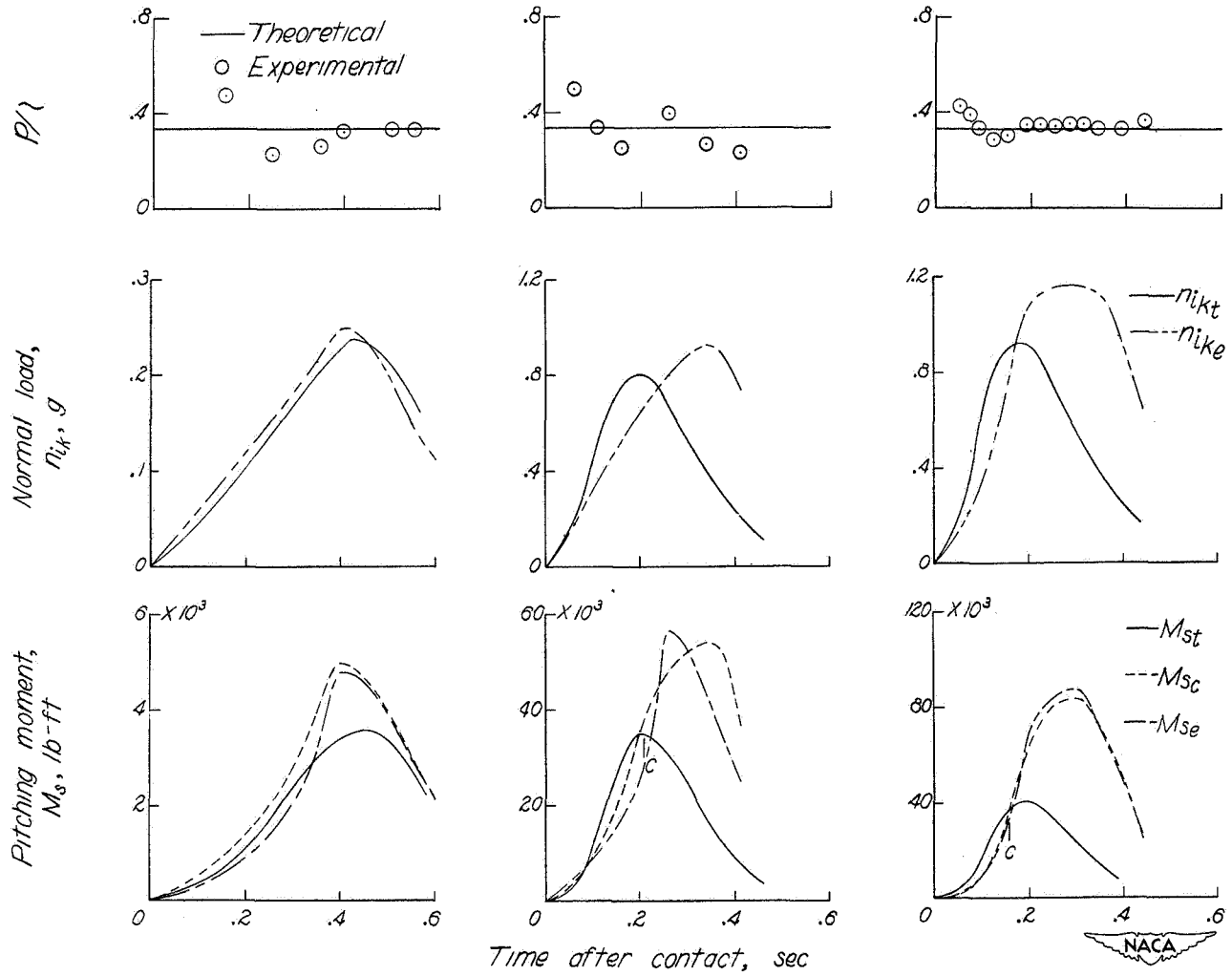

(a) Run 3. ω_o = 1° per second. (b) Run 5. ω_o = 0° per second. (c) Run 7. ω_o = −4.9° per second.

Figure 8.– Comparison of experimental and theoretical ratio of center of pressure to wetted keel length, normal loads, and pitching moments including effects of chine immersion and initial rotation.

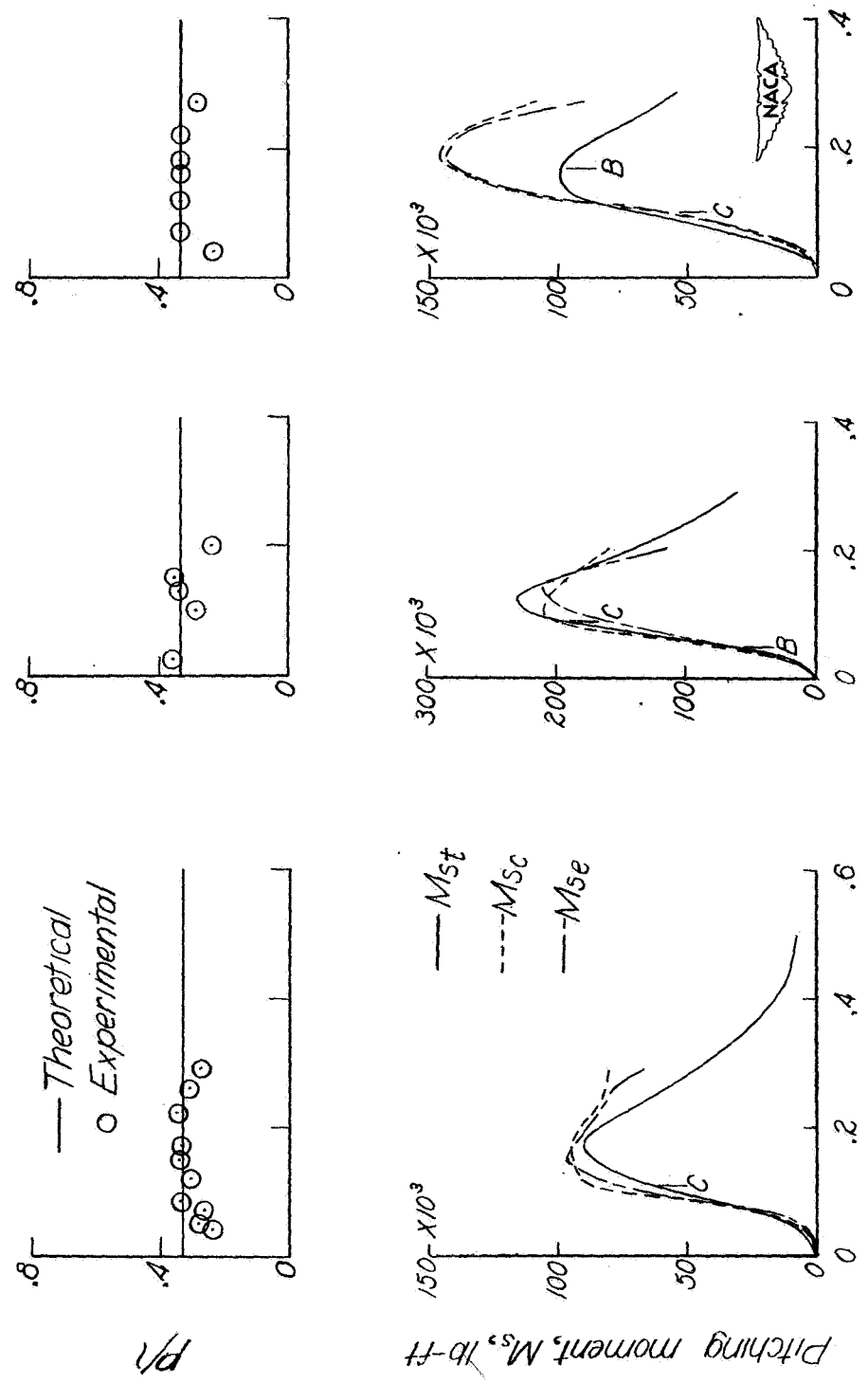

(a) Run 2. (b) Run 12. (c) Run 13.

Figure 9.- Comparison of experimental and theoretical ratio of center of pressure to wetted keel length and pitching moments.

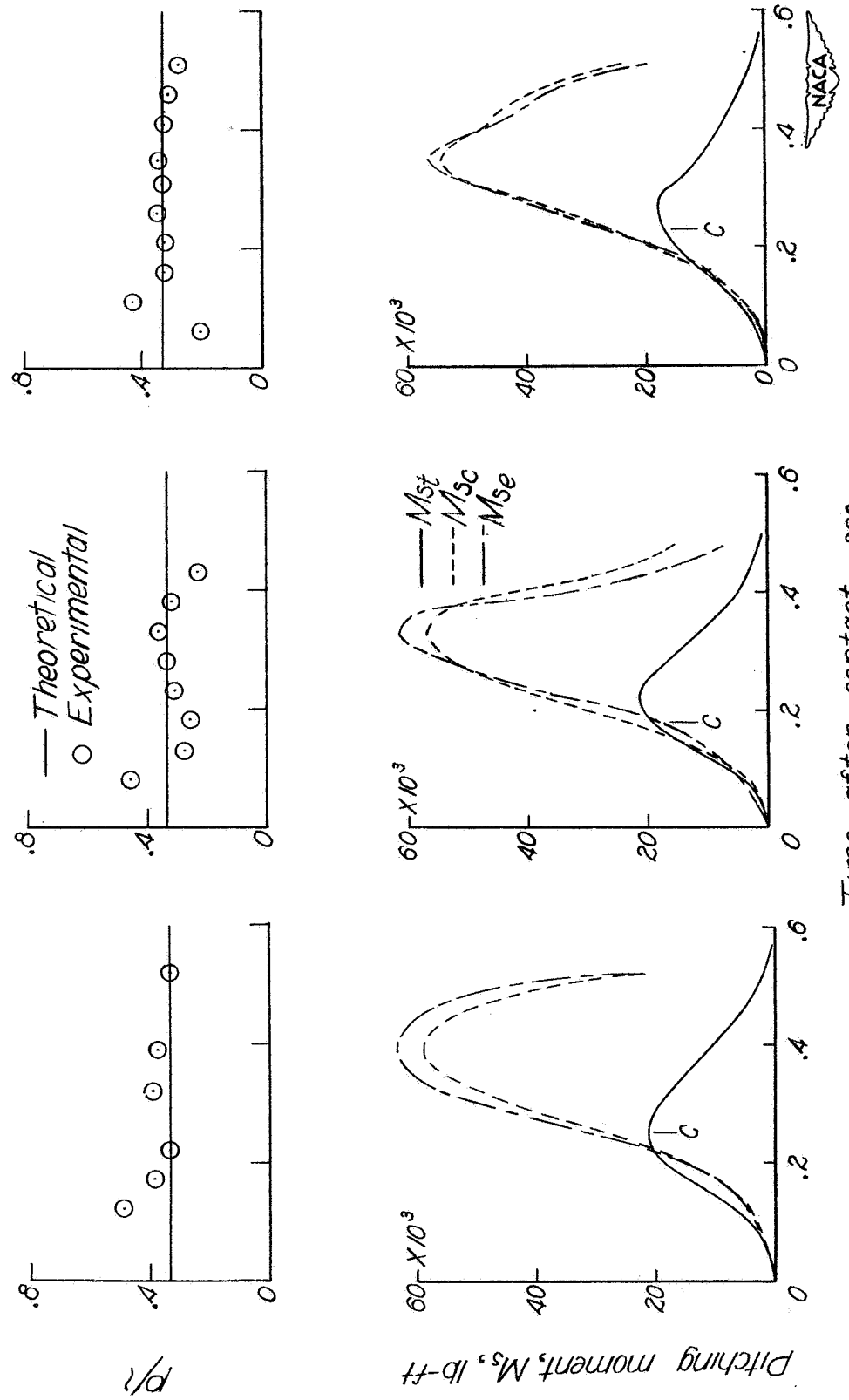

(d) Run 9.

(e) Run 10.

(f) Run 11.

Figure 9.- Concluded.